View metadata, citation and similar papers at core.ac.uk

brought to you by CORE

provided by Carolina Digital Repository

Biochem. J. (2004) **379**, 449–459 (Printed in Great Britain)

online data

Mutations in and near the second calcium-binding domain of integrin αIIb affect the structure and function of integrin αIIbβ3

Susan GIDWITZ*[1], Brenda TEMPLE† and Gilbert C. WHITE, II*‡

*Division of Hematology and Oncology, Department of Medicine, Center for Thrombosis and Hemostasis, University of North Carolina, Chapel Hill, NC 27599-7035, U.S.A., †R. L. Juliano Structural Bioinformatics Core Facility and Department of Biochemistry and Biophysics, University of North Carolina, Chapel Hill, NC 27599-7260, U.S.A., and ‡Department of Pharmacology, University of North Carolina, Chapel Hill, NC 27599-7035, U.S.A.

Calcium-binding domains in the α-subunit of integrins contain a central loop structure. To examine the importance of the loop structure, a series of αIIb mutants containing changes to the calcium-liganding amino acids have been constructed. Significantly, none of the mutant αIIbβ3 complexes was detected on the surface of transfected cells, but mutant pro-αIIb was detected in cell lysates in complex with β3. To study the importance of the regions flanking the second calcium-binding domain for ligand-binding and ligand-binding specificity, three αIIb/α5 chimaeras containing α5 sequences flanking or flanking and including the second calcium-binding domain were constructed. The chimaera containing both α5-flanking regions was not expressed on the cell surface, but FR1 and FR2, substituting either the first or second flanking region, were expressed. FR1β3-transfected cells lost the ability to adhere to fibrinogen and to support aggregation and had minimal fibrinogen-binding ability. The heterodimer complex was less stable than the wild-type. FR2β3-transfected cells adhered to fibrinogen and bound soluble fibrinogen with higher affinity when compared with wild-type. In addition, the heterodimer complex was more stable than wild-type. These results indicate that the conformation of the second calcium-binding domain is critical for maturation of the αIIbβ3 complex and expression on the cell surface and that the surrounding sequences are critical for αIIbβ3 function.

Key words: calcium-binding domain, fibrinogen, integrin αIIbβ, integrin αIIbβ3, platelet.

INTRODUCTION

Integrins are a family of heterodimeric cell-surface proteins, which mediate cell–cell and cell–extracellular matrix and cell–soluble ligand interactions [1]. The platelet integrin αIIbβ3 (GPIIb-IIIa) is the major cell-surface protein at approx. 80 000 copies/platelet [2], representing approx. 15 % of the surface protein [3]. αIIbβ3 plays an essential role in primary haemostasis, mediating platelet–platelet and platelet–subendothelial matrix interactions through the binding of its ligands fibrinogen, von Willebrand factor, fibronectin and vitronectin [4,5].

Integrins are synthesized from separate gene products on chromosome 17 [6,7] in the calcium-rich environment of the endoplasmic reticulum, where αIIb is synthesized as a single polypeptide chain precursor of M_r 145 000 and forms a non-covalent heterodimer with the β3-subunit [8–11]. Preliminary glycosylation takes place before the heterodimer is transported to the Golgi apparatus, where endoproteolytic cleavage of αIIb into disulphide-bonded heavy and light chains and oligosaccharide processing to complex carbohydrates occurs [11,12].

Each of the α- and β-subunits consists of a large extracellular domain, a transmembrane region and a short (except for β4) cytoplasmic tail. The α-subunits contain four highly conserved bivalent cation-binding domains that were originally modelled to be structurally similar to the 'EF-hand' motif found in calmodulin and other proteins [13,14], but are now modelled to be nine-aminoacid β-hairpin loops with the consensus sequence Asp-Hpb-Asp/Asn-Xaa-Asp/Asn-Gly-Hpb-Xaa-Asp, where Hpb represents a hydrophobic residue [15,16]. Both heterodimer association and ligand binding are dependent on bivalent-cation binding [17,18]. Calcium binds to the α-subunit of αIIbβ3, and high-affinity binding of fibrinogen requires that all four calcium-binding sites be occupied [19].

Using structural modelling, Springer [15] proposed a β-propeller secondary structure for the N-terminal approx. 440 amino acids of α-integrins. The model consists of a circular array of seven repeats of four β-strands separated by loops. In this model, ligand and Mg^{2+} binding are predicted to be on the upper face of the β-propeller, whereas the four calcium-binding domains are proposed to lie in loops between strands 1 and 2 of repeats 4–7 and be orientated near the bottom of the propeller. This model has been recently confirmed by the solving of the crystal structure of extracellular domain of the αVβ3 complex [16].

Although the β-propeller model and crystal structure model ligand binding to be at the interface of the upper surface of the β-propeller and the β-subunit, compelling evidence has also implicated the second calcium-binding domain of αIIb, amino acids 296–314, as being important in the ligand binding. Chemical cross-linking of the fibrinogen γ-chain C-terminal peptide, followed by proteolysis, identified the second calcium-binding domain as a critical region for binding the peptide [20]. High-affinity binding of the peptide required calcium and that αIIbβ3 be in the activated conformation [21]. Peptides corresponding to amino acids 296–306 or 300–312 blocked platelet aggregation and directly bound to fibrinogen. Moreover, antibodies against $\alpha IIb^{296-306}$ blocked binding of fibrinogen to the peptide and to αIIbβ3

Abbreviations used: CHO, Chinese-hamster ovary-K1; DMEM, Dulbecco's modified Eagle's medium; DTT, dithiothreitol; HRP, horseradish peroxidase; mAb, monoclonal antibody; WT, wild-type.

[1] To whom correspondence should be addressed, at 932 Mary Ellen Jones Bldg., CB 7035, Chapel Hill, NC 27599-7035, U.S.A. (e-mail gidwitz@med.unc.edu).

© 2004 Biochemical Society

[22,23]. In a previous study [24], we showed that chimaeric receptors in which all or parts of the second calcium-binding domain were replaced with the highly homologous α5 sequence demonstrated no difference in expression or function of the receptor. In the present study, we have examined the importance of the calcium-binding loop structure and surrounding sequences on protein expression and function by constructing a series of point mutations in the second calcium-binding domain of αIIb and by making chimaeras with α5 that contained the second calcium-binding domain and the sequences flanking it, or just each of the flanking sequences.

MATERIALS AND METHODS

Construction of mutant αIIb cDNA clones

To facilitate cloning, the *Not*I–*Cla*I fragment of αIIb was subcloned into Bluescript II KS and named BSIIbN/C. All mutants were constructed using a PCR mutagenesis technique. For all mutations, the upstream primer was the mutagenic primer. Mutagenic oligonucleotides created the amino acid change(s) designated in the name of the clone and contained a restriction site near the 5′-end of the oligonucleotide unique to the BSIIbN/C. For D297A ($Asp^{297} \rightarrow Ala$), N299A, D297A-N299A and D297Q-N299Q, the mutagenic oligonucleotide spanned the *Bsm*I site at nt 964 of αIIb. For D301A and D305A, the oligonucleotide spanned the *Aat*II site at nt 987. The downstream primer spanned the *Cla*I site at nt 1374. The PCR product was digested with either *Bsm*I or *Aat*II and *Cla*I and subcloned into BSIIbN/C.

αIIb/$\alpha5_{(254\text{-}348)}$ was constructed by ligating a PCR product from αIIb with one from α5. The αIIb PCR product spanned the *Pml*I site at nt 737 and made two silent mutations to create an *Asc*I site at base 859, bordering the upstream non-conserved region flanking the second calcium-binding domain. The α5 PCR product contained an *Asc*I near the 5′-end, followed immediately by an α5 sequence from nt 906–1190. A silent mutation was introduced at nt 1191 to destroy the *Xcm*I site. The 3′-end of the PCR product matched the sequence of αIIb from nt 1154–1185, including the *Xcm*I site at nt 1170. The PCR products were digested with *Pml*I and *Asc*I or *Asc*I and *Xcm*I respectively, and ligated into BSIIbN/C that had been digested with *Pml*I and *Xcm*I.

FR1 was constructed by ligating the αIIb *Pml*I–*Asc*I PCR product with a PCR product of α5 that spanned the *Asc*I site and bases 906–977, followed by αIIb sequence from nt 938 to the *Bsm*I site at nt 964 of αIIb into BSIIbN/C that had been digested with *Pml*I and *Bsm*I. FR2 was similarly constructed using an αIIb PCR product that spanned the *Bsm*I site through the *Hae*II site at nt 1019 and an α5 PCR product that included αIIb sequence from the *Hae*II site through nt 1038 and then α5 sequence through the *Xcm*I site, as above. The appropriately digested PCR products were ligated into BSIIbN/C that had been digested with *Hae*II and *Xcm*I. The sequence of each of the mutant clones was confirmed, and the *Not*I–*Cla*I fragment of each mutant was then subcloned into wild-type pRcCMVαIIb [24].

Cell culture and transfections

COS-7 cells were obtained from the UNC Tissue Culture Facility and maintained in DMEM (Dulbecco's modified Eagle's medium; high glucose formula) containing 10 % (v/v) foetal bovine serum and 1 % penicillin and streptomycin. Wild-type or mutant constructs were co-transfected with pcDNA1/Ampβ3ΔE, a β3 construct containing a silent mutation to remove the internal *Eco*RI site, into COS-7 cells using LIPOFECTAMINE™ (Gibco BRL, Gaithersburg, MD, U.S.A.) as described previously [24]. CHO (Chinese-hamster ovary-K1) cells were maintained and transfected by electroporation as described previously [25].

Antibodies

The mAb (monoclonal antibody) Tab, [26], specific for αIIb, was provided by R. P. McEver (University of Oklahoma Health Sciences Center, Oklahoma City, OK, U.S.A.). The mAb B1B5 [27], which recognized a membrane-proximal epitope on αIIb, was provided by J. S. Bennett (University of Pennsylvania, Philadelphia, PA, U.S.A.). Anti-β3 mAb AP3 [28] and rabbit polyclonal anti-αIIb SEW-8 were provided by P. J. Newman (Blood Center of Southeastern Wisconsin, Milwaukee, WI, U.S.A.). The αIIbβ3-complex-specific mAbs AP2 [29], 10E5 [30] and A2A9 [31] were supplied by T. J. Kunicki (Scripps Research Institute, La Jolla, CA, U.S.A.), B. S. Coller (Albert Einstein University, New York, NY, U.S.A.) and J. S. Bennett respectively. The activating mAb LIBS 6, specific for β3 [32], was supplied by M. H. Ginsberg (Scripps Research Institute). PAC-1 murine IgM [33] was from University of Pennsylvania Cell Center (Philadelphia, PA, U.S.A.). FITC–PAC-1 was from BD Biosciences (San Jose, CA, U.S.A.). mAbs against synthetic peptides containing the N- and C-terminal fibrinogen Aα RGD motifs (Aα 87–100 and Aα 566–680 respectively) were provided by Z. M. Ruggeri (Scripps Research Institute) [34]. mAb 4A5 [35] against the fibrinogen γ-chain H12 sequence was provided by G. R. Matsueda (Bristol–Myers Squibb Pharmaceutical Research Institute, Princeton, NJ, U.S.A.). Function-blocking anti-hamster $\alpha5\beta1$ mAb PB1 [36] was a gift from R. L. Juliano (University of North Carolina). HRP (horseradish peroxidase)-conjugated goat anti-rabbit IgG was from Sigma (St. Louis, MO, U.S.A.). FITC-goat anti-mouse IgG and rabbit anti-mouse IgM were from Zymed (San Francisco, CA, U.S.A.), FITC-chicken anti-fibrinogen was from Biopool International (Ventura, CA, U.S.A.); rabbit anti-fibronectin was from Chemicon International (Temecula, CA, U.S.A.). R-phycoerythrin-conjugated donkey anti-rabbit IgG $F(ab')_2$ was from Jackson Immunoresearch (West Grove, PA, U.S.A.).

Immunoprecipitation

Cells were immunoprecipitated essentially as described previously [24]. Briefly, cells were solubilized in a buffer containing 1 % Nonidet P40 (Sigma) and protease inhibitors. Cellular debris was removed by centrifugation and lysates were precleared with normal mouse serum (Sigma) and GammaBind Plus Sepharose (Amersham Biosciences, Piscataway, NJ, U.S.A.). Cleared lysates were incubated for 1 h at 4 °C with the indicated mAb, followed by GammaBind Plus Sepharose and then washed five times in 50 mM Tris/HCl (pH 8), 0.5 % Nonidet P40 and 0.5 M NaCl. Before lysis, a portion of the cells was incubated with NHS-LC-biotin [succinimidyl-6-(biotinamido)hexanoate; Pierce, Rockford, IL, U.S.A.] to label the cell-surface proteins as described previously [24]. Biotinylated immunoprecipitates were separated on 7.5 % non-reducing SDS/polyacrylamide gel, electrotransferred to nitrocellulose (Costar, Cambridge, MA, U.S.A.), detected with streptavidin–HRP (Gibco BRL) and visualized by chemiluminescence using either ECL® or ECL Plus™ (Amersham Biosciences) or SuperSignal™ CL-HRP (Pierce). Unlabelled proteins were separated by SDS/PAGE (7.5 % gel) under reducing conditions, transferred to either nitrocellulose or PVDF (Millipore, Bedford, MA, U.S.A.), immunodetected with SEW-8 followed by goat anti-rabbit-HRP and visualized by chemiluminescence. Biotinylated molecular-mass standards (Sigma) were included on gels.

© 2004 Biochemical Society

Flow cytometry

Flow-cytometric analysis was performed as described previously [25]. Briefly, cells were harvested, washed and resuspended in PBC [PBS containing 2 % (w/v) BSA, 0.1 mM $CaCl_2$ and 0.1 mM $MgCl_2$]. Cells were incubated at the indicated temperature for the indicated time with the indicated antibody, washed, incubated with FITC-goat anti-mouse IgG, washed, fixed with paraformaldehyde and analysed on a flow cytometer. PAC-1-binding studies were conducted as described previously [24] using unlabelled PAC-1 and FITC-rabbit anti-mouse IgM or with FITC–PAC-1, except that cells were activated either by incubation with DTT (dithiothreitol) or with LIBS 6. For studies on subunit dissociation, cells were harvested and washed and then resuspended in PBS containing 2 % BSA. Immediately before the start of the experiment, EDTA was added to a final concentration of 5 mM. Cells were incubated at the indicated temperature for the indicated times, and then immediately diluted 10-fold with PBS, centrifuged and resuspended in PBC containing the αIIbβ3-complex-specific mAb AP2 and processed as above.

Adhesion

Adhesion was performed as described previously [24]. Fibrinogen was either purified from fresh-frozen plasma using the glycine-precipitation method of Kazal et al. [37] or purchased from Enzyme Research Laboratories (South Bend, IN, U.S.A.). Fibrinogen was treated with gelatin–agarose three times (Sigma) to remove contaminating fibronectin. For adhesion studies, flat-bottomed immunoassay plates (Costar, Corning, Acton, MA, U.S.A.) were incubated overnight at 4 °C either with 10 μg/ml fibronectin (Collaborative Biomedical Products, Becton Dickinson, Bedford, MA, U.S.A.) or with the indicated concentration of fibrinogen and then blocked with heat-inactivated BSA. Cells (1×10^5) were allowed to adhere to wells of the ligand-coated plates for 2 h at 37 °C. Plates were washed, stained with Crystal Violet and absorbance was determined at 540 nm. Non-specific binding was defined as binding to heat-inactivated BSA-coated wells. When present, the peptide GRGDSF (University of North Carolina Protein Chemistry Laboratory) was incubated with the cells for 30 min before plating.

Fibrinogen and fibronectin binding

Immediately before use, fibrinogen was centrifuged at 14 000 ***g*** for 5 min to reduce the potential amount of fibrin in the preparation. For fibrinogen-binding studies, cells were resuspended in DMEM + 20 mM Hepes (pH 7.5), LIBS 6 ascites at a 1:100 dilution and either 1 mM GRGDSF or buffer. Cells were incubated at room temperature (23 °C) for 15 min before the addition of FITC-fibrinogen [24]. Cells were incubated at room temperature for 30 min, washed, fixed and analysed by flow cytometry. Specific binding was defined as the difference in mean fluorescent intensity between cells incubated in the presence and absence of GRGDSF. Results were fitted to the 1-site ligand-binding equation, $y = a_0x/(a_1 + x)$. To test the effect of the anti-N-terminal and anti-C-terminal fibrinogen Aα RGD motif and anti-γ chain antibodies, cells were resuspended in Hepes/Tyrode's buffer without calcium or magnesium that had been treated with Chelex-100 (Bio-Rad, Hercules, CA, U.S.A.). Calcium was added to a final concentration of 2 mM. Cells were incubated with LIBS 6 and either 1 mM GRGDSF or buffer for 15 min at room temperature before the addition of 50 nM fibrinogen and 10 μg/ml anti-fibrinogen N-terminal-Aα antibody, anti-C-terminal-Aα RGD antibody, anti-γ-chain H12 antibody or control IgG, all of them purified earlier from ascites on GammaBind Sepharose. Cells were incubated at 22 °C for 30 min, washed and then incubated with FITC-chicken anti-human fibrinogen. Cells were washed, fixed and analysed by flow cytometry as above.

Fibronectin binding was measured by resuspending harvested cells in Hepes/Tyrode's containing 1 mM $MnCl_2$. Cells were incubated with 66 μg/ml PB1 and 1 mM GRGDSF, 31 μM cyclic RGDFV (Bachem, Torrance, CA, U.S.A.; underlining indicates the D form) or buffer for 15 min before addition of 100 nM fibronectin. Cells were incubated at room temperature for 30 min, washed and incubated with rabbit anti-fibronectin followed by R-phycoerythrin-conjugated donkey anti-rabbit IgG $F(ab')_2$, fixed and analysed by flow cytometry.

Aggregation

Aggregation was performed essentially as described previously [24]. Cells were harvested, washed and resuspended at 2×10^7 cells/ml in Hepes/Tyrode's (pH 7.4) containing 1 mM $MnCl_2$, but without calcium or magnesium, and incubated with 1 mM GRGDSF or buffer for 15 min at room temperature. Fibrinogen was added to a final concentration of 0.25 mg/ml, and cells were incubated on a gyratory shaker at 75 rev./min for 30 min at room temperature and then photographed.

Molecular modelling

Models of wild-type αIIb, FR1 and FR2 were built and optimized using the Modeler module of the InsightII 2000 molecular modelling system from Accelrys (http://www.accelrys.com). Sequences for α5 (human, mouse and frog), αV (human, bovine, mouse, chick, newt and frog), α8 (human, mouse and chick) and αIIb (human, mouse, dog, rabbit, pig, horse and yellow baboon) from the RGD group of integrins were obtained from Swiss-Prot and TrEMBL [38] and aligned using ClustalX [39]. The structural template used for modelling was the αV chain of the crystal structure of the αVβ3 complex (PDB Identifier 1JV2) [16]. Panels in Figures 1, 10 and 11 were created with SPOCK [40] and rendered with MOLSCRIPT [41] and Raster3D [42,43].

RESULTS

Expression of calcium-binding domain mutant complexes

We prepared a series of mutant αIIb DNAs encoding single amino acid changes at the calcium liganding sites, substituting Ala or Gln for the wild-type Asp or Asn, creating the following mutant αIIb constructs: D297A, N299A, D301A and D305A, and double mutants, D297A-N299A and D297Q-N299Q (Figure 1). αIIb mutants were transiently co-expressed with β3 and cell-surface expression was examined by immunoprecipitation of biotinylated cell-surface proteins with antibodies to αIIb. Bands corresponding to αIIb and β3 were detected in cells transfected with wild-type αIIb, but no bands were seen in mock-transfected cells, cells transfected with β3 only or cells transfected with any of the mutants (Figure 2A, lanes 1–9), indicating that mutant αIIbβ3 constructs were not expressed on the cell surface.

Unlabelled cell lysates were immunoprecipitated with B1B5, an mAb to a membrane-proximal epitope of αIIb that is not altered by the mutations, to evidence intracellular protein expression. As can be seen in Figure 2(B), no protein was detected in mock-transfected cells or cells transfected with β3 only. Cells transfected with wild-type αIIb expressed both mature and pro-αIIb, the uncleaved precursor to αIIb. Each of the mutant transfectants expressed pro-αIIb in quantities similar to cells expressing wild-type αIIbβ3, but did not express any of the mature form.

© 2004 Biochemical Society

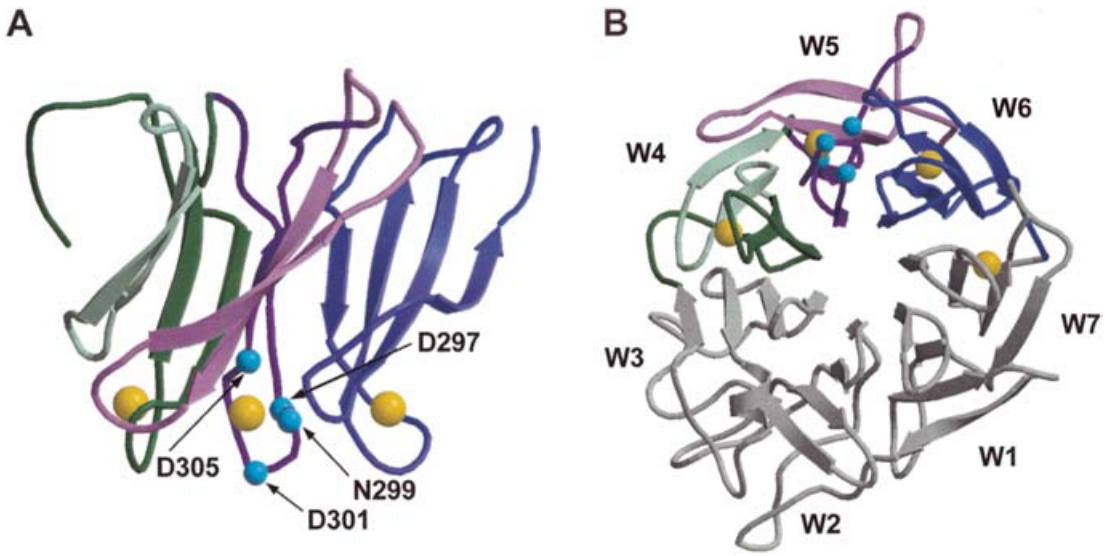

Figure 1 Model of αIIb β-propeller depicting location of second calcium-binding domain point mutations and flanking regions 1 and 2 (FR1 and FR2)

(**A**) Side view of β-propeller blades 4–6 (dark green, dark plum and violet respectively). Calcium co-ordinating amino acids that were mutated are depicted as light blue balls. Light green indicates FR1 and light plum indicates FR2. Gold balls indicate calcium atoms. (**B**) Bottom view of β-propeller. Colours as in (**A**).

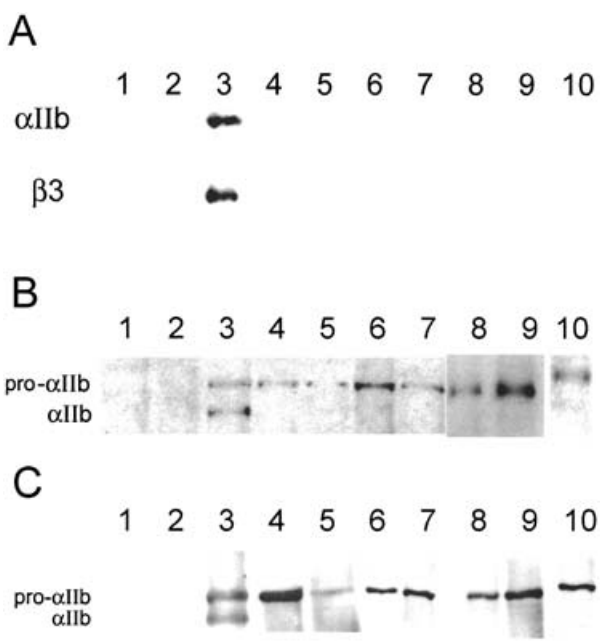

Figure 2 Expression, processing and complex formation of mutant integrins

Cells were transiently co-transfected with WT (wild-type) or mutant α-subunit and with β3, and after 72 h they were analysed for cell surface and cellular expression of integrins. (**A**) Cell-surface proteins were biotinylated and immunoprecipitated with anti-αIIb mAb B1B5, electrophoresed and detected with streptavidin–HRP as described in the Materials and methods section. 1, mock; 2, β3; 3, WT; 4, D297A-N299A; 5, D297Q-N299Q; 6, D297A; 7, N299A; 8, D301A; 9, D305A; 10, $\alpha IIb/\alpha 5_{(254\text{-}353)}$. (**B**) Cell lysates were immunoprecipitated with B1B5, electrophoresed and immunodetected with anti-αIIb polyclonal antibody SEW-8 as described in the Materials and methods section. Lanes as in (**A**). (**C**) Lysates were immunoprecipitated with anti-β3 mAb AP3, electrophoresed and immunodetected with SEW-8 as above. Lanes as in (**A**).

We examined whether the mutant α-subunits were capable of complexing with β3 by immunoprecipitating cell lysates with AP3, an mAb to β3, and detecting with a polyclonal antibody to αIIb, SEW-8. No protein was detected in either mock-transfected cells or cells transfected with β3 only. Mature αIIb and a small amount of pro-αIIb were detected in cells transfected with wild-type αIIb. When lysates from cells transfected with mutant αIIb were examined, a band corresponding to pro-αIIb was seen, indicating that mutant pro-αIIb proteins were capable of complexing with β3. For D301A and D305A, faint bands were seen corresponding to mature αIIb, suggesting that small amounts of these mutant proteins were being processed (Figure 2C, lanes 1–9).

Expression of flanking region chimaeras

Three chimaeras were constructed in which α5 sequences were substituted for αIIb sequences in the regions directly flanking the second calcium-binding domain: $\alpha IIb/\alpha 5_{(254\text{-}353)}$, a chimaera that substitutes the sequence from just distal to the first calcium-binding domain, through the second calcium-binding domain and immediately up to the beginning of the third calcium-binding domain with the corresponding sequence of α5; FR1, a chimaera that substitutes the sequence between the first and second calcium-binding domains of αIIb with the corresponding sequence of α5; and FR2, a chimaera that substitutes the sequence between the second and third calcium-binding domains of αIIb with the corresponding sequence of α5 (Figure 1B).

No $\alpha IIb/\alpha 5_{(254\text{-}353)}$–β3 complex was detected on the cell surface (Figure 2A, lane 10). When unlabelled cell lysates were immunoprecipitated with B1B5, only uncleaved pro-αIIb, but not the mature form, was detected (Figure 2B, lane 10). When the lysates were immunoprecipitated with AP3 and probed with an αIIb-specific antibody, the uncleaved form of $\alpha IIb/\alpha 5_{(254\text{-}353)}$ was detected, indicating that $\alpha IIb/\alpha 5_{(254\text{-}353)}$ complexed with β3 (Figure 2C, lane 10).

Immunoprecipitation of biotinylated cell-surface proteins with Tab from transiently transfected COS cells expressing FR1 and FR2 revealed that the α-subunit of each mutant protein was expressed on the cell surface (Figure 3). For FR2, a similar amount of β3 co-immunoprecipitated with the FR2 α-subunit, indicating heterodimer complex formation. Interestingly, almost no β3 co-immunoprecipitated with the FR1 α-subunit, suggesting either that FR1 exists on the cell surface as an isolated subunit or that

© 2004 Biochemical Society

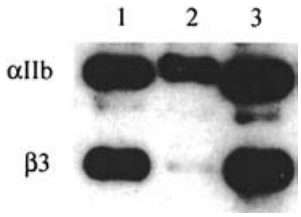

Figure 3 Expression and complex formation of FR1 and FR2 in COS cells

Cell-surface proteins were biotinylated and immunoprecipitated with anti-αIIb mAb Tab, electrophoresed and detected with streptavidin–HRP as described in the Materials and methods section. 1, WT; 2, FR1; 3, FR2.

Table 1 Antibody binding to stable clones of CHO-transfected cells

Stable cell lines expressing β3, WT, FR1 or FR2 were incubated with anti-αIIb mAb Tab or with complex-specific mAb AP2, washed and stained with FITC-labelled goat anti-mouse IgG and analysed by flow cytometry.

	Tab	AP2	100× AP2	1000× AP2
β3	1.3	2.4	3.2	11.1
WT	411.6	301.3	441.1	541.3
FR1	235.7	24.9	40.3	45.3
FR2	305.0	318.0	–	–

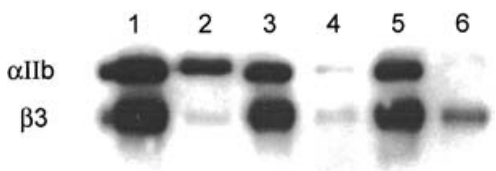

Figure 4 Differential co-immunoprecipitation of FR1 with β3 using subunit- and complex-specific mAbs

Cell-surface proteins from CHO-stable cell lines expressing WT (lanes 1, 3 and 5) or FR1 (lanes 2, 4 and 6) were labelled with biotin and immunoprecipitated with Tab (lanes 1 and 2), complex-specific mAb AP2 (lanes 3 and 4) or AP3 (lanes 5 and 6), electrophoresed and detected with streptavidin–HRP.

the non-covalent association between the α- and β-subunits is not strong enough to survive solubilization and immunoprecipitation.

Stable CHO cell lines expressing FR1 and FR2 were generated and compared with previously made CHO cell lines expressing wild-type αIIbβ3, mock-transfected and β3-only transfected cells. Flow cytometry with Tab showed FR1 and FR2 expression levels that were 50–75 % of wild-type (Table 1). Staining with AP2, a complex-specific mAb, revealed that wild-type and FR2 expressing cells had nearly equal staining (301 versus 318 arbitrary units), but FR1 staining was < 10 % of wild-type (25 units). All subsequent experiments were performed using the stable cell lines.

To investigate further the state of FR1 on the cell surface, solubilization was performed with a variety of detergents, including Brij96, digitonin and *n*-octyl glucoside, and in the presence or absence of calcium, magnesium, manganese or GRGDSF. None of these conditions significantly increased the amount of β3 that co-immunoprecipitated with FR1 (results not shown). Similar results were obtained when immunoprecipitation was performed with the β3-specific mAb AP3. The wild-type α-subunit co-immunoprecipitated with β3 in nearly equimolar amounts, but little or no FR1 was co-immunoprecipitated (Figure 4). When immunoprecipitation was performed with ten times the normal

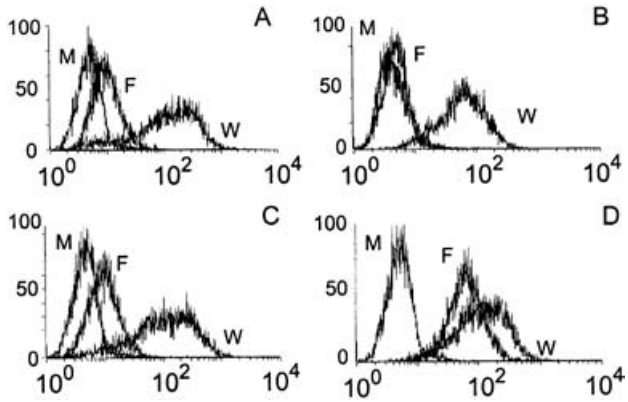

Figure 5 Flow-cytometric analysis of cell-surface expression of FR1 subunit- and complex-specific mAbs

Stable cell lines expressing WT (W), FR1 (F) or mock-transfected cells (M) were incubated with complex-specific mAbs AP2, A2A9, 10E5 or with anti-αIIb mAb Tab, washed and stained with FITC-labelled goat anti-mouse IgG and analysed by flow cytometry. (**A**) AP2, (**B**) A2A9, (**C**) 10E5 and (**D**) Tab.

concentration of AP2, a small amount of FR1β3 complex was immunoprecipitated, but it only represented a small fraction of the total FR1 present on the cell surface (Figure 4). These results suggest the presence of two forms of FR1β3, one that is recognized by AP2 and one that is not.

Further studies were performed using flow cytometry with several complex-specific mAbs. FR1β3 reacted weakly with AP2 and 10E5, but not with A2A9, while reacting strongly with the αIIb-specific mAb Tab (Figure 5). Incubations were performed with mAb concentrations that were saturating for cells expressing wild-type αIIbβ3. For both AP2 and 10E5, only a single population of FR1β3 was detected, indicating that all cells expressed both forms of FR1β3, rather than some cells expressing integrin that recognized the mAbs and some cells expressing integrin that did not recognize mAbs. Several attempts were made to increase the amount of binding of AP2 to FR1β3. Incubations with AP2 were performed at 4, 25 and 37 °C for 1, 4 or 24 h in an attempt to trap the complex in a conformation capable of binding an antibody, or with antibody at 100- and 1000-fold higher concentrations to determine if the low antibody binding was due to a decreased affinity of FR1β3 for AP2. None of these conditions increased antibody binding to FR1β3 expressing cells by more than a factor of 2, which was similar to the increase in AP2 binding to wild-type cells under the same conditions (Table 1 and results not shown), suggesting a large change in affinity of FR1β3 for AP2 or a lack of complex formation.

Adhesion studies

As an initial attempt to determine whether FR1 and FR2 had any change in their function, the ability of wild-type or mutant integrin-expressing CHO cells to adhere to fibrinogen immobilized on the wells of microtitre plates was examined. CHO cells constitutively express α5β1, the prototypic fibronectin receptor, and all three cell lines adhered to fibronectin-coated wells with similar efficiency (results not shown). Adhesion on fibrinogen over a 1000-fold concentration range was examined and results were normalized to adhesion on fibronectin. Adhesion on both fibronectin and fibrinogen was blocked by GRGDSF (results not shown). As can be seen in Figure 6, maximal adhesion of wild-type cells on fibrinogen was approx. 70 % of adhesion on fibronectin and occurred when the coating concentration was

© 2004 Biochemical Society

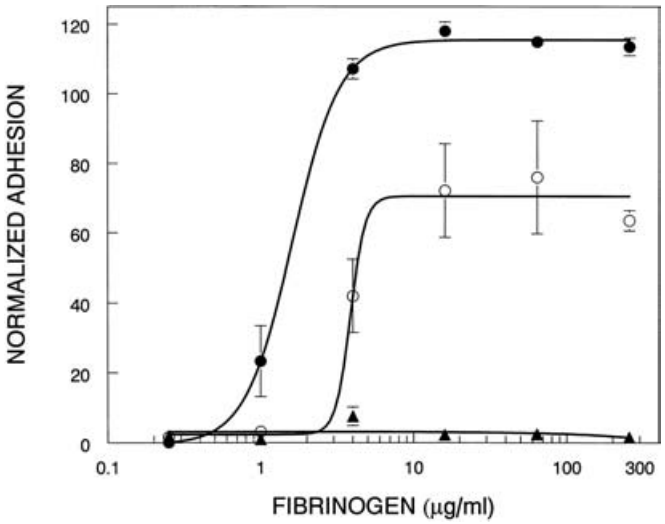

Figure 6 Comparison of WT, FR1 and FR2 adhesion on fibrinogen

Microtitre plates were coated with 10 μg/ml fibronectin or the indicated concentration or fibrinogen and blocked with BSA. Cells were allowed to attach for 2 h at 37 °C, washed and the number of bound cells was quantified by staining with Crystal Violet. Background binding was subtracted (binding to BSA). Adhesion on fibronectin was defined as 100 for each cell line, and adhesion on fibrinogen was normalized to fibronectin binding. Adhesion on fibronectin was similar for each cell line. ○, WT; ▲, FR1; ●, FR2.

<10 μg/ml fibrinogen. Half-maximal adhesion occurred when the coating concentration was 3.7 μg/ml fibrinogen. Although FR1β3-expressing cells adhered normally to fibronectin, they did not adhere to fibrinogen-coated wells, even when the coating concentration was 256 μg/ml, nearly 70 times the half-maximal coating concentration for wild-type cells. Whereas wild-type cells adhered to fibronectin better than fibrinogen, FR2β3-expressing cells adhered to fibrinogen even better when compared with fibronectin. As a result, maximal normalized adhesion of FR2β3 cells on fibrinogen was 164 % of wild-type. Half-maximal adhesion occurred at 1.9 μg/ml fibrinogen, approximately half that of wild-type.

Soluble ligand binding

We examined the ability of the mutant integrins to bind soluble ligands. Neither mock-transfected nor β3-only cells were able to bind soluble ligand when activated with either LIBS 6 or DTT (results not shown). FR1 was not able to bind to the ligand mimetic antibody PAC-1 when integrin was activated either with the activating mAb LIBS 6 or with DTT, whereas both wild-type and FR2 bound similar amounts of PAC-1 when activated with LIBS 6 (Figure 7A). Wild-type and FR2 bound only minimal amounts of PAC-1 in the absence of LIBS 6, demonstrating that the FR2 chimaera was not in a constitutively active state. FR1 bound only minimal amounts of fibrinogen even when incubated with 2000 nM fibrinogen, a concentration more than ten times the value of K_d for fibrinogen for wild-type (results not shown), suggesting that only the fraction of FR1β3 that was recognized by AP2 was able to bind fibrinogen. Besides fibrinogen, αIIbβ3 can bind several soluble ligands, including fibronectin [4,5]. We examined whether FR1 retained the ability to bind fibronectin, even though its ability to bind fibrinogen was impaired, and determined that fibronectin binding was impaired in a fashion similar to fibrinogen binding (results not shown).

FR2 bound fibrinogen in a manner similar to wild-type, but with higher affinity (Figure 7B). The maximal binding was statistically identical: 15.2 ± 1.0 and 14.8 ± 0.45 arbitrary units for wild-type and FR2 respectively. However, FR2 had a higher affinity for fibrinogen, having a K_d value of 66.2 ± 6.4 nM versus 148 ± 25 nM for wild-type ($P < 0.005$). Even though FR2 was a chimaera with α5, which, when complexed with β1, binds fibrinogen through an RGD sequence [44], the binding of fibrinogen by FR2 was mediated by the C-terminus of the fibrinogen γ-chain, as binding was inhibited by antibodies to the H12 sequence of the γ-chain, but not by antibodies to either

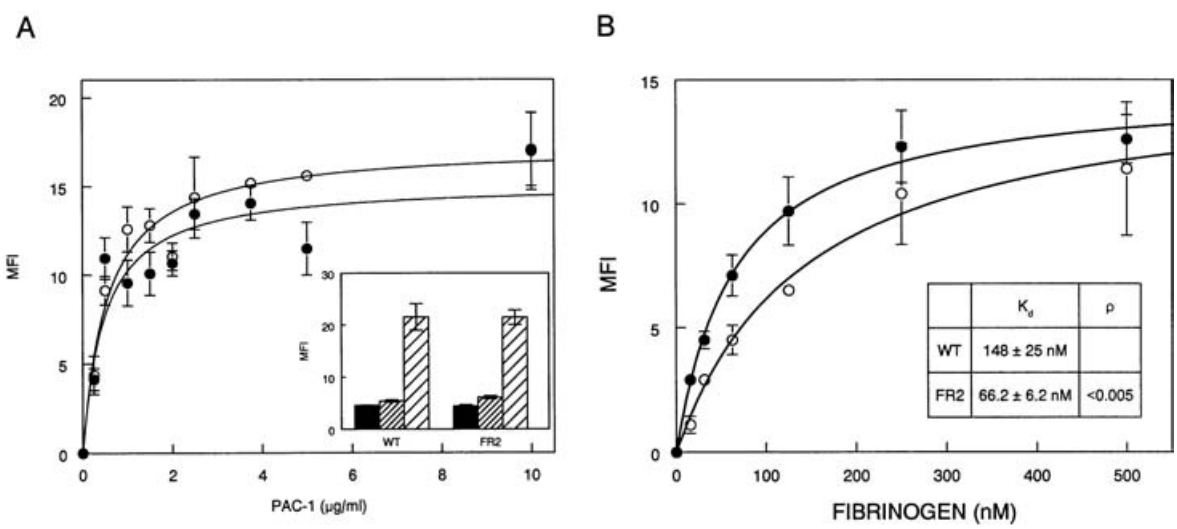

Figure 7 PAC-1 and fibrinogen binding to FR2 and WT

(**A**) PAC-1 binding. Specific binding of PAC-1 was measured by incubating cells with LIBS 6-activating antibody either in the presence or absence of 1 mM GRGDSF. FITC–PAC-1 was added at the indicated final concentration and cells were incubated for 30 min at room temperature, washed, fixed and analysed by flow cytometry. Specific binding was defined as total binding minus ligand binding in the presence of GRGDSF. ○, WT; ●, FR2. MFI, mean fluorescent intensity. Inset: cells were incubated with 10 μg/ml FITC–PAC-1. Black bar, binding in the presence of LIBS 6 and 1 mM GRGDSF; narrow diagonal lines, binding without addition of LIBS 6; wide diagonal lines, binding in the presence of LIBS 6. (**B**) Specific binding of fibrinogen was measured by incubating cells with LIBS 6 activating antibody either in the presence or absence of 1 mM GRGDSP. FITC–fibrinogen was added at the indicated final concentration, and cells were incubated for 30 min at room temperature, washed, fixed and analysed by flow cytometry. Specific binding was defined as FITC–fibrinogen binding minus FITC–fibrinogen binding in the presence of GRGDSP. ○, WT; ●, FR2.

© 2004 Biochemical Society

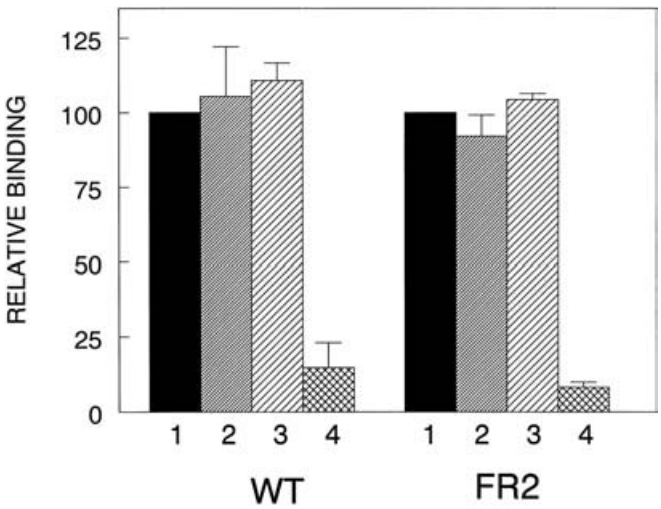

Figure 8 Inhibition of fibrinogen binding to both WT and FR2 by antibodies to the γ-chain of fibrinogen, but not by antibodies to the RGD sequences

Cells were incubated with LIBS 6 for 15 min at room temperature. Cells were then incubated for 30 min at room temperature with 50 nM fibrinogen and 10 μg/ml control or anti-fibrinogen IgG. Cells were washed and then incubated with FITC-chicken anti-human fibrinogen IgG for 30 min at room temperature, washed, fixed and analysed by flow cytometry. Specific binding was defined as fibrinogen binding minus binding in the presence of 1 mM GRGDSF peptide. Specific fibrinogen binding in the presence of control IgG was set at 100. 1, control IgG; 2, anti-Aα chain N-terminal RGD IgG; 3, anti-Aα chain C-terminal RGD IgG; 4, anti-γ chain H12 IgG. Inhibition by the anti-γ-chain H12 IgG was significantly different from control IgG ($P < 0.001$) in each case.

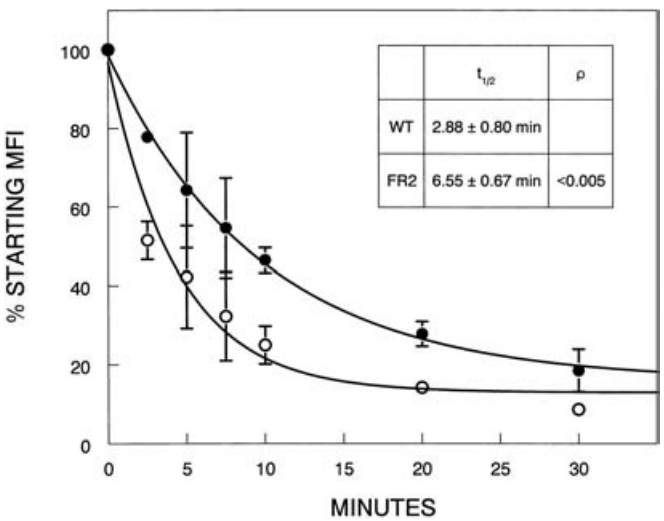

Figure 9 Greater resistance to subunit dissociation by EDTA in FR2 compared with WT

Cells were incubated with 5 mM EDTA at 37 °C for the indicated time, washed, incubated with AP2, washed again and incubated with FITC-goat anti-mouse IgG, washed once more, fixed and then analysed by flow cytometry. Each curve in the Figure is the average of three separate experiments. ○, WT; ●, FR2. MFI, mean fluorescent intensity.

of the Aα chain RGD sequences (Figure 8). Thus, binding of fibrinogen to FR2, which is through an RGD mechanism, was not mediated by α5β1, and substitution of the α5 sequence into αIIb did not alter the mechanism by which the chimaeric αIIbβ3 bound fibrinogen. Confirming the fibrinogen-binding studies, FR2 formed large aggregates in the presence of fibrinogen when activated with $MnCl_2$, as did wild-type cells, but FR1 was not able to form aggregates (results not shown).

Dissociation studies

The αIIbβ3 complex irreversibly dissociates when incubated with EDTA at 37 °C, and subunit dissociation can be monitored by loss of AP2 binding. We have demonstrated previously a correlation between the stability of chimaeric αIIbβ3 complexes and fibrinogen binding: mutants that bound fibrinogen with higher affinity than wild-type had increased stability, whereas mutants with lower binding were less stable [24]. We examined the stability of FR2β3 complexes compared with wild-type when incubated with 5 mM EDTA at 37 °C for 30 min (Figure 9). Wild-type αIIbβ3 had a dissociation half-time of 2.88 ± 0.80 min, equal to the previously determined half-time of 2.56 ± 0.07 min [24], whereas FR2 had a dissociation half-time of 6.55 ± 0.67 min ($P < 0.005$).

DISCUSSION

We have previously demonstrated that the second calcium-binding domain of αIIb could be replaced by the corresponding sequence of α5 with no measurable effect on expression or function, but certain point mutations that substituted the α5 sequence for αIIb within the second calcium-binding domain had subtle effects on receptor function [24]. In the present study, we constructed a series of αIIb/α5 chimaeras to study the importance of the regions flanking the calcium-binding domain on receptor expression and function. Calcium-binding domains are regions of high homology; αIIb and α5 have 80% sequence identity over 34 amino acids that include the calcium-binding domain and immediate flanking regions. The remaining 61 amino acids in the region between the first and second and the second and third calcium-binding domains, designated FR1 and FR2 respectively, share low homology. In the β propeller model, the flanking regions occupy strands C and D of the blade preceding and containing the calcium-binding domain, regions which are farther from the central axis and are proposed to accommodate sequence modifications such as in the alternatively spliced integrins α3, α6 and α7 or, in our case, the αIIb/α5 chimaeras [15]. The chimaera with the greatest substitution of α5 sequence, $\alpha IIb/\alpha5_{(254\text{-}353)}$, a chimaera that substituted α5 sequence for αIIb from immediately after the end of the first calcium-binding domain to the beginning of the third calcium-binding domain, however, was not expressed on the cell surface, but complexed with the β3-subunit. In contrast, chimaeras that substituted individual regions, FR1 or the second calcium-binding domain or FR2 were expressed on the cell surface.

Two populations of FR1 were expressed on the surface of CHO cells. The minor one (5–20% of the population recognized by the αIIb-specific mAb Tab) recognized certain αIIbβ3 complex-specific mAbs and formed a heterodimer that was stable when immunoprecipitated, whereas the major one (80–95% of the total) did not. It is not clear whether the population of FR1 that did not recognize complex-specific antibodies had undergone a conformational change that simply ablated the epitope or if the complex had dissociated. It has been reported that a point mutation at L264A, which is within the FR1 chimaeric region, resulted in the expression of αIIbβ3 on the cell surface, but the heterodimer was not recognized by a variety of antibodies, suggesting that a major conformational change was induced by the mutation [45]. Although heterodimer formation is required for transport to the cell surface [10,12,46,47], an unstable αIIbβ3 complex has been described previously [48].

The presence of two populations of FR1, with presumably the same amino acid sequence, could be explained by an equilibrium

© 2004 Biochemical Society

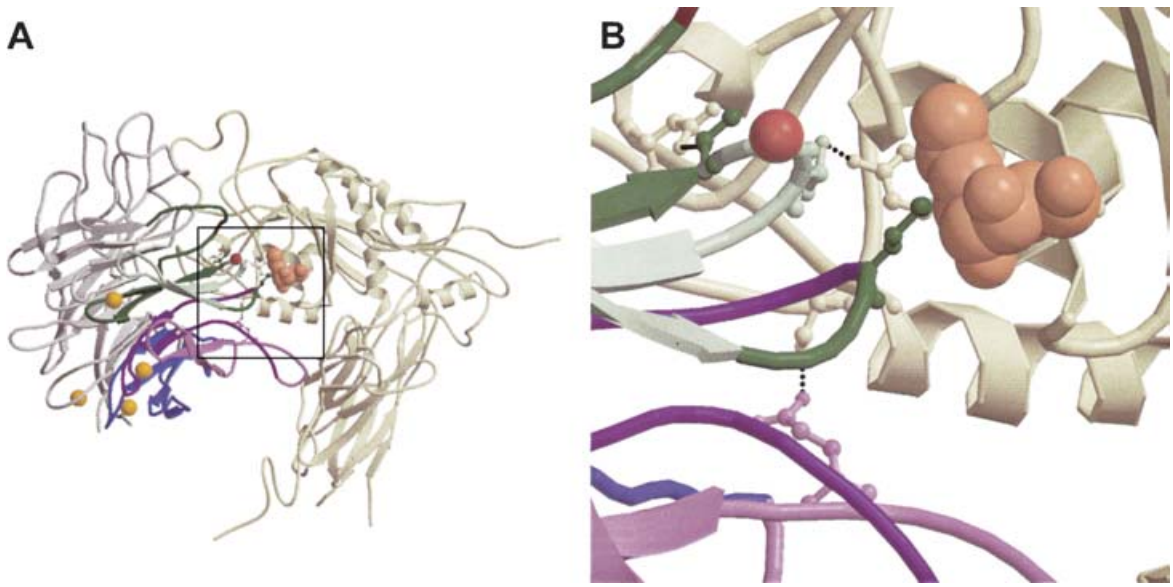

Figure 10 Model of a portion of αIIbβ3 depicting the interaction of mutated regions αIIb with β3

Colours of αIIb are as in Figure 1; $\beta 3_{55-432}$, tan; N-linked carbohydrate, large brown balls (for clarity, only the first *N*-acetylglucosamine subunit is indicated). A red ball indicates a potential N-linked glycosylation site. Amino acids participating in intersubunit hydrogen-bondings are indicated by ball-and-stick models (dark green, Thr^{260}; light green, Thr^{264}; light violet, Glu^{322}). Hydrogen bonds are indicated by black dotted lines. Met^{272} is shown in dark green by a ball-and-stick model. Asp^{232} of the RGD-binding pocket is indicated in dark red: (**A**) overview; (**B**) close-up of amino acids participating in intersubunit interactions and potential glycosylation sites.

between two states, a properly folded one and an improperly folded conformation. An alternative explanation of the different populations is differential glycosylation. The α5 FR1 sequence contains three potential N-linked glycosylation sites, and the FR1 α-subunit immunoprecipitated with an anti-αIIb-subunit-specific mAb migrated at a slightly higher apparent molecular mass than did the subunit immunoprecipitated with a complex-specific mAb, suggesting differential glycosylation as the probable reason for the two states. Of the three potential glycosylation sites, the last one is homologous with one in αV, and would not be expected to cause conformational problems. Molecular modelling of αIIb and FR1, based on the crystal structure of αV [16], suggests that the second potential glycosylation site, an NGS sequence, is mostly buried, and therefore is probably not utilized. The first potential glycosylation site, NLT, at amino acids 261–263, is in a loop at the top of the β-propeller and in contact with the β-subunit. The residues are mostly exposed and could be utilized. Importantly, Thr^{263} is conserved in αv, α5 and αIIb and participates in intersubunit hydrogen-bonding (Figure 10). It is also adjacent to the Leu^{264} that has been shown to be critical for proper conformation of the complex [45] and close to Thr^{260}, which also participates in intersubunit hydrogen-bonding. Additionally, the crystal structure of αvβ3 reveals that the glycosylation site at Asn^{320} of the β-subunit is utilized, is close to Asn^{263} of the α-subunit, and interacts with the α-subunit through hydrophobic interactions with conserved Met^{272}. The corresponding sequence in β1 does not have a glycosylation site, suggesting that to maintain the proper conformation of the complex, either the site on the α-subunit or the β-subunit should be glycosylated, but not both. Glycosylation has been demonstrated to be essential for stable integrin subunit association by Zheng et al. [49], who reported that limited deglycosylation of K562 cells or purified α5β1 in liposomes led to the formation of an unstable complex that dissociated after immunoprecipitation. The importance of glycosylation in subunit interactions has also been recently demonstrated for the formation of a stable triple-helix structure in collagens [50].

The small amount of ligand bound by FR1 is consistent with the smaller, presumably properly glycosylated, population which is recognized by certain function-blocking complex-specific antibodies, as being active, and the larger, improperly glycosylated population as being inactive. Differential glycosylation has been shown to affect both the expression level and the ability of α5β1 and α6β1 to bind to fibronectin and laminin respectively [51,52].

Whereas the major population of FR1 forms a weak or perturbed complex with β3, FR2 forms a highly stable complex. The dissociation half-time for FR2 when incubated with EDTA at 37 °C is more than twice that of wild-type αIIbβ3. FR2β3 would appear to be a 'super' αIIbβ3, adhering to fibrinogen better, having a higher affinity for fibrinogen and being more stable. The FR2 region encompasses three variable loop regions and two highly conserved strands (Figure 11). The first nine and last four residues of the FR2 substitution lie in two juxtaposed loops on the top of the FR2 β-propeller and are within 25 Å (1 Å = 0.1 nm) of the βA and EGF (epidermal growth factor) domains of β3 in the complex. In the αVβ3 complex, the first loop makes one hydrogen bond to the β3-subunit between the side chains of αVQ311 and β3S291. A glutamic residue is invariant at this position among the RGD clade (αIIb, αV, α5 and α8) (see Figure 11 and Supplemental Figure 1, http://BiochemJ.org/bj/379/bj3790449add.htm), and this interaction is expected to be maintained in the αIIbβ3, α5β1 and FR2β3 complexes. Although close to the β-subunit, the residues of the third loop of FR2 are predicted not to make hydrogen bonds with the β3-subunit. While there are a significant number of differences between αIIb and α5 in these two loops in FR2 on the top of the β-propeller, the one hydrogen-bond contact between αV and β3 in the unliganded complex is, not surprisingly, conserved within the entire RGD clade. It is possible that substituting the α5 loops for the αIIb loops on the top of the β-propeller might result in a complex that has higher affinity for fibrinogen and adheres to fibrinogen better, but it is not at all clear how a substitution in those loops alone could account for the formation of a more stable

© 2004 Biochemical Society

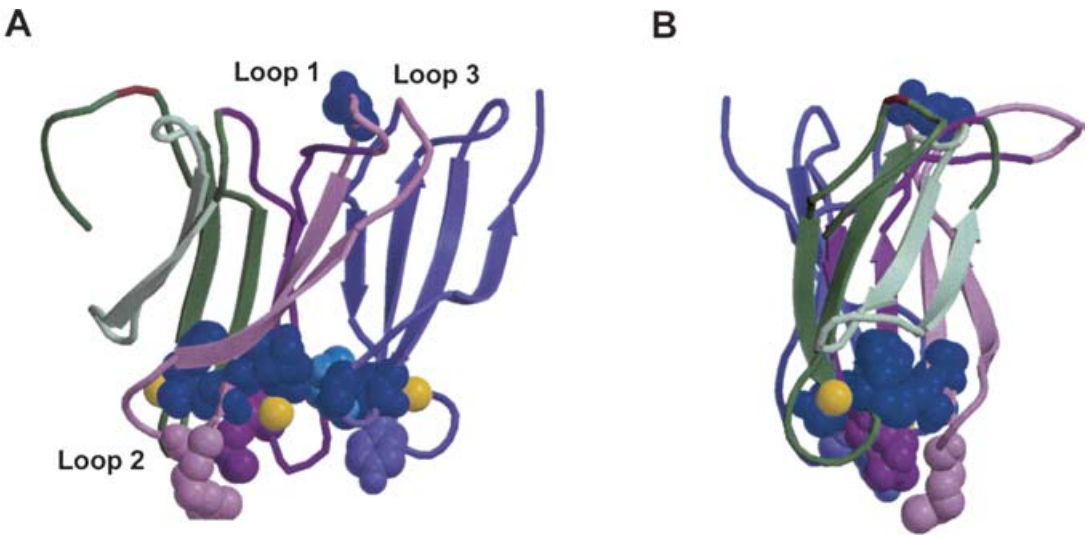

Figure 11 Model of blades 4–6 of αIIb β-propeller highlighting important conserved and variable amino acids

(**A**) Blade colours and calcium atoms as in Figure 1. Dark blue CPK model, invariant amino acids; light blue, conserved residues; light plum, highly variable. Conserved large hydrophobic amino acid at the 7th position of calcium-binding loop 3 is shown by a violet CPK model. The arginine residue at position 7 of the second calcium-binding domain is shown by a dark plum CPK model. Arginine of loop 2 is shown as light plum. (**B**) Model rotated by 90° about the vertical axis.

complex when incubated with EDTA, since the calcium-binding sites are on the bottom of the β-propeller.

The second loop in FR2 lies near the second calcium-binding domain and near the site of our previously reported 'super' αIIbβ3, LD (R303H304 $\rightarrow$ L303D304 mutation at the 7th and 8th positions of the second calcium-binding domain) [24]. The consensus sequence for the β-hairpin calcium-binding loops includes a conserved hydrophobic amino acid at the 7th position in the loop with the carbonyl oxygen of this hydrophobic residue co-ordinating the calcium atom. This residue is conserved as a large hydrophobic amino acid across the 2nd, 3rd and 4th calcium-binding sites in all 19 species of the α-integrins in the RGD clade for which there is sequence (see Supplemental Figure 2, http://www.BiochemJ.org/bj/379/bj3790449add.htm). The striking exception to the consensus sequence is the highly charged arginine that is found in the 7th position of the second calcium-binding loop in each of the seven sequenced species of αIIb. Given the strong conservation of a large hydrophobic residue at the 7th position of the β-hairpin calcium-binding loop, it is possible that a single-point mutation of arginine to leucine would also give the same functional behaviour as FR2 and the RH $\rightarrow$ LD substitution did. Since the side chain of the residue at the 7th position is largely solvent-exposed and can easily tolerate being charged and polar without major structural changes, it seems probable that the positively charged side chain acts by destabilizing calcium binding. Potential serendipitous interactions between the α5 loop 2 sequence of FR2 and the arginine residue in the αIIb second calcium-binding domain could mimic, partially or completely, the proposed stabilization of calcium binding seen with the LD substitution. The closest residues to the arginine residue in the second calcium-binding loop are a proline–arginine in loop 3 in αIIb. In FR2, these positions are histidine–proline, which may induce either a conformational change or a change in the electrostatic potential of the second calcium-binding site. This hypothesis seems reasonable, given the noted importance of bivalent cation binding on both heterodimer association and high-affinity ligand binding [17–19], and is supported further by the constrained structural relationship of the calcium-binding sites indicated by the near invariance of the band of residues at the bottom of the β-propeller (blue balls in Figure 11).

Integrin activation involves global rearrangement of the structure. The crystal structure of the resting integrin predicts a 'bent' conformation, with the ligand-binding site at the interface of the α- and β-subunits occluded, and activation is supposed to cause straightening of the molecule. Conflicting models posit that the head groups separate on activation [53,54] or that the legs separate [55–57]. As a result of the legs separating, the first loop of FR2 is modelled such that no contact is made with the β-subunit. It is possible that changes in the FR2 loop facilitate breaking of the hydrogen bond between the subunits, but we did not see either constitutive or increased activation of FR2β3, but found only increased affinity for fibrinogen.

Our results indicate that the conformation of the second calcium-binding loop is critical for maturation and cell-surface expression of αIIbβ3, but not for the formation of the αIIbβ3 heterodimer. Each of the point mutations that we made to calcium co-ordinating residues in the second calcium-binding domain blocked expression of the heterodimer on the cell surface, but none of them blocked interaction with β3. The mutations, however, altered the complex and the complexes did not undergo normal post-translational modification. After complex formation, the nascent heterodimer is normally transported to the *trans*-Golgi where cleavage of the α-chain into heavy and light chains occurs [12,58,59]. Although each of the mutants formed heterodimers, only pro-αIIb was detected in immunoprecipitates from whole cell lysates, indicating lack of proteolytic processing in the Golgi. Recently, two new mutations V298F and I374T that occur in the second and third calcium-binding domains respectively, which cause Glanzmann's thrombasthenia, have been studied [60]. Similar to the results that we present, both mutations allowed αIIbβ3 complex formation to occur; however, each mutation caused decreased, rather than absent, surface expression of the complex. Molecular modelling predicted the necessity for branched-chain hydrophobic amino acids at these positions to maintain the tight β turns necessary for the proper conformation of the calcium-binding loops.

© 2004 Biochemical Society

In conclusion, we have demonstrated the importance of the conformation of the second calcium-binding domain for cell-surface expression of the αIIbβ3, but not for heterodimer formation, and the surrounding sequences are critical for αIIbβ3 assembly and function.

This study was supported by National Institute of Health grant HL45100.

REFERENCES

1 Hynes, R. O. (1992) Integrins: versatility, modulation, and signaling in cell adhesion. Cell (Cambridge, Mass.) **69**, 11–25

2 Wagner, C. L., Mascelli, M. A., Neblock, D. S., Weisman, H. F., Coller, B. S. and Jordan, R. E. (1996) Analysis of GPIIb/IIIa receptor number by quantification of 7E3 binding to human platelets. Blood **88**, 907–914

3 Jennings, L. K. and Phillips, D. R. (1982) Purification of glycoproteins IIb and III from human platelet plasma membranes and characterization of a calcium-dependent glycoprotein IIb–III complex. J. Biol. Chem. **257**, 10458–10466

4 Phillips, D. R., Charo, I. F., Parise, L. V. and Fitzgerald, L. A. (1988) The platelet membrane glycoprotein IIb–IIIa complex. Blood **71**, 831–843

5 Plow, E. F. and Ginsberg, M. H. (1989) Cellular adhesion: GPIIb-IIIa as a prototypic adhesion receptor. Prog. Hemost. Thromb. **9**, 117–156

6 Sosnoski, D. M., Emanuel, B. S., Hawkins, A. L., van Tuinen, P., Ledbetter, D. H., Nussbaum, R. L., Kaos, F. T., Schwartz, E., Phillips, D., Bennett, J. S. et al. (1988) Chromosomal localization of the genes for the vitronectin and fibronectin receptors α subunits and for platelet glycoproteins IIb and IIIa. J. Clin. Invest. **81**, 1993–1998

7 Bray, P. F., Barsh, G., Rosa, J. P., Luo, X. Y., Magenis, E. and Shuman, M. A. (1988) Physical linkage of the genes for platelet membrane glycoproteins IIb and IIIa. Proc. Natl. Acad. Sci. U.S.A. **85**, 8683–8687

8 Bray, P. F., Rosa, J. P., Lingappa, Y. W., Kan, R. P. and McEver, R. P. (1986) Biogenesis of the platelet receptor for fibrinogen: evidence for separate precursors for glycoproteins IIb and IIIa. Proc. Natl. Acad. Sci. U.S.A. **83**, 1480–1484

9 Duperray, A., Troesch, A., Berthier, R., Chagnon, E., Frachet, P., Uzan, G. and Marguerie, G. (1989) Biosynthesis and assembly of platelet GPIIb-IIIa in human megakaryocytes: evidence that assembly between pro-GPIIb and GPIIIa is a prerequisite for expression of the complex on the cell surface. Blood **74**, 1603–1611

10 O'Toole, T. E., Loftus, J. C., Plow, E. F., Glass, A. A., Harper, J. R. and Ginsberg, M. H. (1989) Efficient surface expression of platelet GPIIb-IIIa requires both subunits. Blood **74**, 14–18

11 Kolodziej, M. A., Vilaire, G., Gonder, D., Poncz, M. and Bennett, J. S. (1991) Study of the endoproteolytic cleavage of platelet glycoprotein IIb using oligonucleotide-mediated mutagenesis. J. Biol. Chem. **266**, 23499–23504

12 Rosa, J. P. and McEver, R. P. (1989) Processing and assembly of the integrin, glycoprotein Iib–IIIa in HEL cells. J. Biol. Chem. **264**, 12596–12603

13 Marsden, B. J., Shaw, G. S. and Sykes, B. (1990) Calcium binding proteins. Elucidating the contributions to calcium affinity from an analysis of species variants and peptide fragments. Biochem. Cell Biol. **68**, 587–601

14 Tuckwell, D. S., Brass, A. and Humphries, M. J. (1992) Homology modelling of integrin EF-hands. Evidence for widespread use of a conserved cation-binding site. Biochem. J. **285**, 325–331

15 Springer, T. A. (1997) Folding of the N-terminal, ligand-binding region of integrin α-subunits into α β-propeller domain. Proc. Natl. Acad. Sci. U.S.A. **94**, 65–72

16 Xiong, J. P., Stehle, T., Diefenbach, B., Zhang, R., Dunker, R., Scott, D. L., Joachimiak, A., Goodman, S. L. and Arnaout, M. A. (2001) Crystal structure of the extracellular segment of integrin αVβ3. Science **294**, 339–345

17 Galit, J. and Ruoslahti, E. (1988) Regulation of the fibronectin receptor affinity by divalent cations. J. Biol. Chem. **263**, 12927–12933

18 Kirchhofer, D., Grzesiak, J. and Pierschbacher, M. D. (1991) Calcium as a potential physiological regulator of integrin-mediated cell adhesion. J. Biol. Chem. **266**, 4471–4477

19 Gulino, D., Boudignon, C., Zhang, L. Y., Concord, E., Rabiet, M. J. and Marguerie, G. (1992) Ca^{2+}-binding properties of the platelet glycoprotein IIb ligand-interacting domain. J. Biol. Chem. **267**, 1001–1007

20 D'Souza, S. E., Ginsberg, M. H., Burke, T. A. and Plow, E. F. (1990) The ligand binding site of the platelet integrin receptor GPIIb-IIIa is proximal to the second calcium binding domain of its α subunit. J. Biol. Chem. **265**, 3440–3446

21 Andrieux, A., Hudry-Clergeon, G., Ryckewaert, J. J., Chapel, A., Ginsberg, M. H., Plow, E. F. and Marguerie, G. (1989) Amino acid sequences in fibrinogen mediating its interaction with its platelet receptor, GPIIbIIIa. J. Biol. Chem. **264**, 9258–9265

22 D'Souza, S. E., Ginsberg, M. H., Matsueda, G. R. and Plow, E. F. (1991) A discrete sequence in a platelet integrin is involved in ligand recognition. Nature (London) **350**, 66–68

23 Taylor, D. B. and Gartner, T. K. (1992) A peptide corresponding to GPIIb α300–312, a presumptive fibrinogen γ-chain binding site on the platelet integrin GPIIb/IIIa, inhibits the adhesion of platelets to at least four adhesive ligands. J. Biol. Chem. **267**, 11729–11733

24 Gidwitz, S., Lyman, S. and White, G. C. (2000) Expression and function of calcium binding domain chimeras of the integrins αIIb and α5. J. Biol. Chem. **275**, 6680–6688

25 Lyman, S., Gilmore, A., Burridge, K., Gidwitz, S. and White, II, G. C. (1997) Integrin-mediated activation of focal adhesion kinase is independent of focal adhesion formation or integrin activation. J. Biol. Chem. **272**, 22538–22547

26 McEver, R. P., Bennett, E. M. and Martin, M. N. (1983) Identification of two structurally and functionally distinct sites on human platelet membrane glycoprotein IIb–IIIa using monoclonal antibodies. J. Biol. Chem. **258**, 5269–5275

27 Silver, S. M., McDonough, M. M., Vilaire, G. and Bennett, J. S. (1987) The *in vitro* synthesis of polypeptides for the platelet membrane glycoproteins IIb and IIIa. Blood **69**, 1031–1037

28 Newman, P. J., Allen, R. W., Kahn, R. A. and Kunicki, T. J. (1983) Quantitation of membrane glycoprotein IIIa on intact human platelets using the monoclonal antibody, AP-3. Blood **65**, 227–232

29 Pidard, D., Montgomery, R. R., Bennett, J. S. and Kunicki, T. J. (1983) Interaction of AP-2, a monoclonal antibody specific for the human platelet glycoprotein IIb–IIIa complex, with intact platelets. J. Biol. Chem. **258**, 12582–12586

30 Coller, B. S., Peerschke, I. L., Scudder, L. E. and Sullivan, C. A. (1983) A murine monoclonal antibody that completely blocks the binding of fibrinogen to platelets produces a thrombasthenic-like state in normal platelets and binds to glycoproteins IIb and/or IIIa. J. Clin. Invest. **72**, 325–338

31 Bennett, J. S., Hoxie, J. A., Leitman, S. F., Vilaire, G. and Cines, D. B. (1983) Inhibition of fibrinogen binding to stimulated human platelets by a monoclonal antibody. Proc. Natl. Acad. Sci. U.S.A. **80**, 2417–2421

32 Frelinger, III, A. L., Du, X. P., Plow, E. F. and Ginsberg, M. H. (1991) Monoclonal antibodies to ligand-occupied conformers of integrin αIIbβ3 (glycoprotein IIb-IIIa) alter receptor affinity, specificity, and function. J. Biol. Chem. **266**, 17106–17111

33 Shattil, S. J., Hoxie, J. A., Cunningham, M. and Brass, L. F. (1985) Changes in the platelet membrane glycoprotein Iib–IIIa complex during platelet activation. J. Biol. Chem. **260**, 11107–11114

34 Cheresh, D. A., Berliner, S. A., Vicente, V. and Ruggeri, Z. M. (1989) Recognition of distinct adhesive sites on fibrinogen by related integrins on platelets and endothelial cells. Cell (Cambridge, Mass.) **58**, 945–953

35 Taubenfield, S. M., Song, Y., Sheng, D., Ball, E. L. and Matsueda, G. R. (1995) A monoclonal antibody against a peptide sequence of fibrinogen γ chain acts as an inhibitor of factor XIII-mediated crosslinking of human fibrin. Thromb. Haemost. **74**, 923–927

36 Brown, P. J. and Juliano, R. L. (1988) Monoclonal antibodies to distinctive epitopes on the α and β subunits of the fibronectin receptor. Exp. Cell Res. **177**, 303–318

37 Kazal, L. A., Amsel, S., Miller, O. P. and Tocantins, L. M. (1963) The preparation and some properties of fibrinogen precipitated from human plasma by glycine. Proc. Soc. Exp. Biol. Med. **113**, 989–994

38 Boeckmann, B., Bairoch, A., Apweiler, R., Blatter, M. C., Estreicher, A., Gasteiger, E., Martin, M. J., Michoud, K., O'Donovan, C., Phan, I. et al. (2003) The SWISS-PROT protein knowledgebase and its supplement TrEMBL in 2003. Nucleic Acids Res. **31**, 365–370

39 Thompson, J. D., Gibson, T. J., Plewniak, F., Jeanmougin, F. and Higgins, D. G. (1997) The CLUSTAL_X Windows interface: flexible strategies for multiple sequence alignment aided by quality analysis tools. Nucleic Acids Res. **25**, 4876–4882

40 Christopher, J. A. (1998) SPOCK: The Structural Properties Observation and Calculation Kit (Program Manual), The Center for Macromolecular Design, Texas A&M University, College Station, TX

41 Kraulis, P. J. (1991) MOLSCRIPT: a program to produce both detailed and schematic plots of protein structures. J. Appl. Crystallogr. **24**, 946–950

42 Bacon, D. J. and Anderson, W. F. (1991) A fast algorithm for rendering space-filling molecule pictures. J. Mol. Graph. **6**, 219–220

43 Merritt, E. A. and Murphy, M. E. P. (1994) Raster3D Version 2.0, a program for photorealistic molecular graphics. Acta Crystallogr. D **50**, 869–873

44 Suehiro, K., Gailit, J. and Plow, E. F. (1997) Fibrinogen is a ligand for integrin α5β1 on endothelial cells. J. Biol. Chem. **272**, 5360–5366

45 Kamata, T., Tieu, K. K., Irie, A., Springer, T. A. and Takada, Y. (2001) Amino acid residues in the αIIb subunit that are critical for ligand binding to integrin αIIbβ3 are clustered in the β-propeller model. J. Biol. Chem. **276**, 44275–44283

46 Duperray, A., Berthier, R., Chagnon, E., Ryckewaert, J. J., Ginsberg, M. H., Plow, E. and Marguerie, G. (1987) Biosynthesis and processing of platelet GPIIb–IIIa in human megakaryocytes. J. Cell Biol. **104**, 1665–1673

© 2004 Biochemical Society

47 Bodary, S. C., Napier, M. A. and McLean, J. W. (1989) Expression of recombinant platelet glycoprotein IIbIIIa results in a functional fibrinogen-binding complex. J. Biol. Chem. **264**, 18859–18862
48 Jackson, D. E., White, M. M., Jennings, L. K. and Newman, P. J. (1998) A Ser162 → Leu mutation within glycoprotein (GP) IIIa (integrin β3) results in an unstable αIIbβ3 complex that retains partial function in a novel form of type II Glanzmann thrombasthenia. Thromb. Haemost. **80**, 42–48
49 Zheng, M., Fang, H. and Hakomori, S. (1994) Functional role of N-glycosylation in α5β1 integrin receptor. De-N-glycosylation induces dissociation or altered association of α5 and β1 subunits and concomitant loss of fibronectin binding activity. J. Biol. Chem. **269**, 12325–12331
50 Bann, J. G., Peyton, D. H. and Bachinger, H. P. (2000) Sweet is stable: glycosylation stabilizes collagen. FEBS Lett. **473**, 237–240
51 Guo, P., Zhang, Y., Zhao, J., Guo, H., Zhang, X. and Chen, H. (2003) Regulation on the expression and N-glycosylation of integrins by *N*-acetylglucosaminyltransferase V. Biochem. Biophys. Res. Commun. **310**, 619–626
52 Chammas, R., Veiga, S. S., Line, S., Potocnjak, P. and Brentani, R. R. (1991) Asn-linked oligosaccharide-dependent interaction between laminin and gp120/140. An α6/β1 integrin. J. Biol. Chem. **266**, 3349–3355
53 Hantgan, R. R., Paumi, C., Rocco, M. and Weisel, J. W. (1999) Effects of ligand-mimetic peptides Arg-Gly-Asp-X (X = Phe, Trp, Ser) on αIIbβ3 integrin conformation and oligomerization. Biochemistry **38**, 14461–14474
54 Liddington, R. C. and Ginsberg, M. H. (2002) Integrin activation takes shape. J. Cell Biol. **158**, 833–839
55 Takagi, J., Petre, B., Walz, T. and Springer, T. A. (2002) Global conformational rearrangements in integrin extracellular domains in outside–in and inside–out signaling. Cell (Cambridge, Mass.) **110**, 599–611
56 Luo, B. H., Springer, T. A. and Takagi, J. (2003) Stabilizing the open conformation of the integrin headpiece with a glycan wedge increases affinity for ligand. Proc. Natl. Acad. Sci. U.S.A. **100**, 2403–2408
57 Mould, A. P., Symonds, E. J., Buckley, P. A., Grossmann, J. G., McEwan, P. A., Barton, S. J., Askari, J. A., Craig, S. E., Bella, J. and Humphries, M. J. (2003) Structure of an integrin–ligand complex deduced from solution X-ray scattering and site-directed mutagenesis. J. Biol. Chem. **278**, 39993–39999
58 Kolodziej, M. A., Vilaire, G., Rifat, S., Poncz, M. and Bennett, J. S. (1991) Effect of deletion of glycoprotein IIb exon 28 on the expression of the platelet glycoprotein IIb/IIIa complex. Blood **78**, 2344–2353
59 Wilcox, D. A., Paddock, C. M., Lyman, S., Gill, J. C. and Newman, P. J. (1995) Glanzmann thrombasthenia resulting from a single amino acid substitution between the second and third calcium-binding domains of GPIIb. Role of the GPIIb amino terminus in integrin subunit association. J. Clin. Invest. **95**, 1553–1560
60 Mitchell, W. B., Li, J. H., Singh, F., Michelson, A. D., Bussel, J., Coller, B. S. and French, D. L. (2003) Two novel mutations in the αIIb calcium-binding domains identify hydrophobic regions essential for αIIbβ3 biogenesis. Blood **101**, 2268–2276

Received 24 April 2003/10 December 2003; accepted 11 December 2003
Published as BJ Immediate Publication 11 December 2003, DOI 10.1042/BJ20030615

© 2004 Biochemical Society